

MODELLING THE MOLECULAR TERMS IN THE TURBULENT HEAT FLUX EQUATION FOR NATURAL CONVECTION

M. Wörner, G. Grötzbach
Institut für Reaktorsicherheit
Forschungszentrum Karlsruhe
Karlsruhe
Germany

ABSTRACT

Direct numerical simulation data for turbulent natural convection in different fluids (liquid sodium, mercury and air) at various Rayleigh numbers are used to investigate the molecular destruction and the molecular diffusion terms in the transport equation of the turbulent heat flux. In modelling the molecular destruction two main results have been obtained. First, it is necessary to include a term in the model which explicitly accounts for the influence of the Prandtl number. Second, a suitable formulation for a model-function which can adequately describe the influence of the turbulence level has to be based on the sum of the turbulence Reynolds and Peclet number. For liquid metals a new approach for modelling the molecular destruction and diffusion in the turbulent heat flux equation is suggested, where both molecular terms are modelled together by approximation of one single term.

INTRODUCTION

Computation of isothermal flows by second moment closure models, which solve the differential transport equations for each component of the turbulent stresses $\overline{u_i u_j}$, has made considerable progress in the past few years and has now reached a level of maturity. However, the situation is not as well satisfactory for non-isothermal buoyant flows. In this case, additional transport equations for the turbulent heat fluxes $\overline{u_j \theta}$, the thermal variance $\overline{\theta^2}$ and half its dissipation rate ϵ_θ need to be solved. The available models for these equations present some important limitations, as shown recently by Hanjalić (1994). Beside other open questions, wall functions for different terms need to be developed and the effects of low Reynolds and Peclet numbers need to be considered. With respect to these topics, detailed information for rather different physical situations is required for both, the behaviour of the molecular terms in the $\overline{u_j \theta}$ -equation and the performance of available models for these terms.

In the present paper, we use results of direct numerical

simulations (DNS) of turbulent convection in different fluids and for different turbulence levels and perform a detailed analysis of the molecular terms in the turbulent heat flux equation. In addition, we analyze some models suggested in literature for closure of these terms. Thus, the scope of the present contribution is to provide reliable data for the molecular terms in the $\overline{u_j \theta}$ equation, to improve the general understanding of the role of these terms, to point out deficiencies of model assumptions, and to suggest improvements.

In the following, we first discuss the Rayleigh-Bénard convection application, give a short introduction to the DNS-code used, and specify the simulations performed. Subsequently, results will be given for the budget of $\overline{u_j \theta}$, including the molecular diffusion and destruction of $\overline{u_j \theta}$. Finally, we analyze models commonly used for closure of these terms and give concluding remarks.

PHYSICAL AND NUMERICAL MODEL

Rayleigh-Bénard Convection

The Rayleigh-Bénard convection is a geometrical simple model which can be used to investigate turbulent heat transfer phenomena in natural convection from a more fundamental point of view. It is given by an infinite fluid layer between two rigid horizontal isothermal walls. The lower one is heated and the upper one is cooled. The physical problem is characterized by two dimensionless numbers: The Rayleigh number $Ra = g\beta\Delta\Theta_W D^3/(\nu\kappa)$ and the Prandtl number $Pr = \nu/\kappa$ (where g = gravity, β = thermal expansion coefficient, $\Delta\Theta_W$ = temperature difference between the walls, D = channel height). Here, three fluids with very different Prandtl numbers are considered: liquid sodium ($Pr = 0.006$), mercury ($Pr = 0.024$), and air ($Pr = 0.71$). The Rayleigh numbers of the simulations span the range $3,000 \leq Ra \leq 630,000$, see Table 1. Though in the liquid metal cases Ra is very low, the Grashof number

$Gr = Ra/Pr$ is in the order of 10^6 . This indicates that the velocity field is fully turbulent.

Simulation Method

In this paper we discuss results for turbulent Rayleigh-Bénard convection which are achieved by the direct simulation method. This means that the full three-dimensional time-dependent conservation equations of mass, momentum, and energy are solved on grids which resolve the largest and smallest scales of turbulence. Thus no statistical turbulence model is used and the simulations do not depend on any model coefficients.

The simulations presented are performed with the TURBIT code (Grötzbach, 1987). This code is based on a finite volume method and allows for direct numerical simulation of turbulent flow and heat transfer in simple channel geometries. With the exception of the buoyancy term, where the Boussinesq approximation is used, the fluid is assumed to be incompressible. The governing equations are solved in dimensionless form. For normalization the channel height D , the velocity $\sqrt{g\beta\Delta\Theta_W D}$, and the temperature difference $\Delta\Theta_W$ are used. Time integration of the momentum equations is performed by the explicit Euler-Leapfrog scheme, whereas for the energy equation the semi-implicit Leapfrog-Crank-Nicolson scheme is used.

For Rayleigh-Bénard convection, periodic boundary conditions in both horizontal directions, x_1 and x_2 , are appropriate to simulate the semi-infinite fluid layer. The horizontal extensions of the channel are selected to $X_{1,2} \approx 8D$ and thus should be large enough to cover even the largest macroscopic scales of the convective layer. At the lower and upper walls, which correspond to $x_3 = 0$ and $x_3 = 1$, respectively, the no slip condition and constant wall temperatures are specified. The numbers of mesh cells N_i used in the equidistantly spaced horizontal directions and in the non-equidistantly spaced vertical direction are given in Table 1.

The simulations listed in Table 1 are the most recently ones of a series of simulations for the same Rayleigh and Prandtl numbers. Starting either from a coarse grid with zero velocities and random temperature fluctuations or from the final data of a simulation with the same Pr but smaller Ra , the results are interpolated to a finer grid and advanced in time. After the flow is fully developed, another interpolation to an even finer grid and additional integration in time is performed until finally a mesh is reached which meets the requirements of a direct simulation of the physical problem. The procedure described drastically reduces the computation time needed to perform the simulations. For a detailed verification of the numerical results for sodium and air see Wörner and Grötzbach (1993a) and Grötzbach (1994). The simulations with mercury are in progress and have not been published up to now.

RESULTS FOR THE $\overline{u_i\theta}$ -EQUATION

Averaging Procedure

In a statistical sense, in turbulent Rayleigh-Bénard convection the horizontal directions x_1 and x_2 are homogeneous. Therefore, for evaluation of statistical quantities averaging is performed over horizontal planes. The resulting vertical profiles $f(x_3)$ are then averaged over several time planes, distributed in the fully developed flow regime. As

Table 1: Parameter and grid data of simulations

Pr	Ra	Gr	$N_{1,2}$	N_3
0.006	3,000	500,000	128	31
0.006	6,000	1,000,000	200	31
0.006	12,000	2,000,000	250	39
0.006	24,000	4,000,000	250	39
0.024	3,000	125,000	128	39
0.024	6,000	250,000	160	39
0.024	12,000	500,000	200	39
0.024	25,000	1,041,667	200	39
0.024	50,000	2,083,333	250	57
0.71	381,000	536,620	180	32
0.71	630,000	887,324	200	39

a consequence of this averaging procedure, the time mean vertical velocity $\overline{u_3}$ is zero and all derivatives of statistical quantities with respect to x_1 and x_2 do vanish.

Transport equation of $\overline{u_3\theta}$

In turbulent Rayleigh-Bénard convection the turbulent heat fluxes in the horizontal directions are zero and only $\overline{u_3\theta}$ exists. With the averaging procedure discussed above, the exact transport equation in dimensionless form for $\overline{u_3\theta}$ reduces to:

$$\begin{aligned} \frac{\partial \overline{u_3\theta}}{\partial t} = & \underbrace{-\overline{u_3^2} \cdot \frac{\partial \Theta}{\partial x_3}}_{P_{3\theta}} + \underbrace{\overline{\theta^2}}_{\phi_{3\theta}} + \underbrace{p \frac{\partial \theta}{\partial x_3}}_{\phi_{3\theta}} \\ & - \underbrace{\frac{\partial}{\partial x_3} \left(\overline{u_3^2\theta} + \overline{p\theta} \right)}_{D_{3\theta,i}} - \underbrace{\frac{1 + Pr}{Pr\sqrt{Gr}} \frac{\partial u_3}{\partial x_i} \cdot \frac{\partial \theta}{\partial x_i}}_{\epsilon_{3\theta}} \\ & + \underbrace{\frac{1}{Pr\sqrt{Gr}} \cdot \frac{\partial}{\partial x_3} \left(\overline{u_3 \frac{\partial \theta}{\partial x_3}} + Pr \theta \frac{\partial \overline{u_3}}{\partial x_3} \right)}_{D_{3\theta,m}} \end{aligned} \quad (1)$$

Here, $P_{3\theta}$ is the production of $\overline{u_3\theta}$. It consists of a contribution due to the mean temperature field (first part of $P_{3\theta}$) and due to buoyancy forces (second part of $P_{3\theta}$). Next, $\phi_{3\theta}$ is the pressure scrambling term and $D_{3\theta,i}$ is the turbulent diffusion. The last two terms are due to molecular effects, i.e. the molecular destruction $\epsilon_{3\theta}$ and the molecular diffusion $D_{3\theta,m}$. In isotropic turbulence $\epsilon_{3\theta}$ is zero and the pressure scrambling term $\phi_{3\theta}$ is the only sink of $\overline{u_3\theta}$.

Budget of $\overline{u_3\theta}$

From our direct numerical simulation data, we calculate each term in the $\overline{u_3\theta}$ -equation and thus evaluate the budget of $\overline{u_3\theta}$. In a previous paper, this was done for the simulations with air ($Ra = 630,000$) and with sodium ($Ra = 24,000$), see Wörner and Grötzbach (1993b). The results indicated that in natural convection the molecular destruction $\epsilon_{3\theta}$ is not zero but is an important sink of turbulent heat flux, at least for low Reynolds or Peclet number flows. The reason is that natural convection is well known to be anisotropic, as it is driven by buoyancy forces.

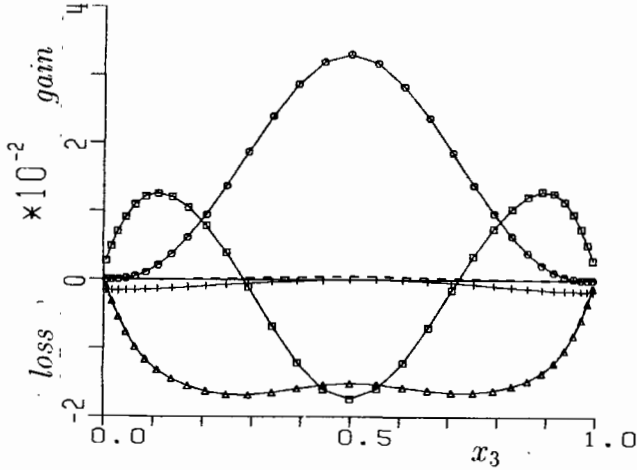


Figure 1: Budget of $\overline{u_3\theta}$ for sodium, $Ra = 3,000$: $D_{3\theta}$ (\square), $P_{3\theta}$ (\circ), $\varepsilon_{3\theta}$ (\triangle), $\phi_{3\theta}$ ($+$), out of balance (---)

In Fig. 1 we present results for the evaluated budget of the $u_3\theta$ -equation for the simulation with sodium and $Ra = 3,000$. First it should be mentioned that for this simulation the Nusselt number is only little bigger than unity. Thus, far most of the heat is transported by conduction and the turbulent heat flux is not really important. Nevertheless, it is worth to study this limiting case and to investigate the budget of $\overline{u_3\theta}$ in some detail. The production $P_{3\theta}$ is zero near the walls and maximum in the centre of the channel. The pressure scrambling term $\phi_{3\theta}$ is very small and the molecular destruction $\varepsilon_{3\theta}$ is the dominant sink term. Fig. 1 shows that $\varepsilon_{3\theta}$ is almost constant in the centre of the layer and decreases in the viscous boundary layers. The diffusive transport $D_{3\theta} = D_{3\theta,t} + D_{3\theta,m}$ redistributes the surplus of $P_{3\theta}$ in the centre of the layer toward the walls. A close inspection of the diffusion $D_{3\theta}$, not shown here, reveals that $D_{3\theta,t}$ is almost zero and thus $D_{3\theta} \approx D_{3\theta,m}$.

With increasing turbulence level, i.e. increasing Rayleigh number, the molecular terms in the $\overline{u_3\theta}$ -equation become less and less important. For air and $Ra = 630,000$ e.g., $D_{3\theta,m}$ is only of relevance in the direct vicinity of the walls, whereas in the centre of the layer this term is negligible and $D_{3\theta} \approx D_{3\theta,t}$. The molecular destruction, however, is not zero even at this Rayleigh number and takes a value of $\varepsilon_{3\theta} \approx \phi_{3\theta}/3$, see Wörner and Grötzbach (1993b).

From these results we conclude that for anisotropic flows, as natural convection, not only modelling of the pressure scrambling term and the turbulent diffusion in the turbulent heat flux equation is essential but also adequate modelling of molecular destruction. In addition, for liquid metals the molecular diffusive transport may not be neglected for most technical applications and needs to be modelled, too.

ANALYSIS OF MODEL ASSUMPTIONS

In this chapter, we use the results of the direct numerical simulations and perform a detailed analysis of models which are suggested in literature for the molecular destruction and molecular diffusion in the turbulent heat flux equation.

Models for the Molecular Destruction

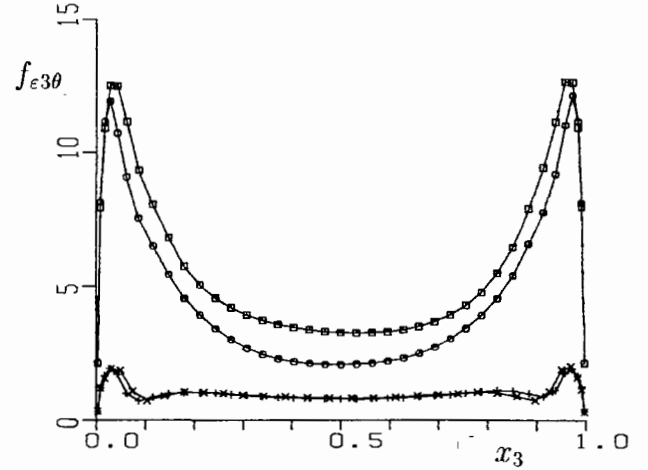


Figure 2: Evaluated profile of function $f_{\varepsilon 3\theta}$. Sodium: $Ra = 12,000$ (\square), $Ra = 24,000$ (\circ); air: $Ra = 381,000$ (\times), $Ra = 630,000$ ($+$).

One possibility to model the molecular destruction $\varepsilon_{i\theta}$ is (Hanjalić, 1994):

$$\varepsilon_{i\theta} = f_{\varepsilon i\theta} \frac{1}{\sqrt{2R}} \frac{\varepsilon}{k} \overline{u_i\theta} \quad (2)$$

Here, k is the turbulent kinetic energy and ε its dissipation rate, and R is the ratio of thermal time scale $\tau_\theta = \overline{\theta^2}/(2\varepsilon_\theta)$ to mechanical time scale $\tau = k/\varepsilon$:

$$R = \frac{\tau_\theta}{\tau} = \frac{\overline{\theta^2}}{k} \frac{\varepsilon}{2\varepsilon_\theta} \quad (3)$$

Hanjalić (1994) suggests $f_{\varepsilon i\theta}$ to be a function of the turbulence Peclet number $Pe_t = k^2/(\kappa\varepsilon)$, which should go to zero at sufficiently high Pe_t and takes the value of unity if Pe_t approaches zero. He emphasizes that an adequate form of this function remains to be specified.

From our direct simulation data, we calculate each quantity in (2) and thus determine the values of function $f_{\varepsilon i\theta}$ for different Rayleigh and Prandtl numbers. In Fig. 2 we show the evaluated vertical profiles of $f_{\varepsilon 3\theta}$ for the simulations with sodium and air for two different Rayleigh numbers in each case. For both simulations with air the value of $f_{\varepsilon 3\theta}$ in the centre of the channel is about 1.2. Though the Rayleigh numbers of both simulations differ by a factor of 1.6, $f_{\varepsilon 3\theta}$ seems to be almost independent of Ra in this range of the Rayleigh number. The increase of Ra only results in a shift of the peaks of $f_{\varepsilon 3\theta}$ toward the walls. This behaviour is directly linked to the thicknesses of the thermal and viscous boundary layers, which decrease as the Rayleigh number increases. The dependence of $f_{\varepsilon 3\theta}$ from the Rayleigh and Prandtl number is much more pronounced for the simulations with sodium, see Fig. 2 again. We identify both, a shift of the peaks of $f_{\varepsilon 3\theta}$ toward the walls and a general decrease of the value of $f_{\varepsilon 3\theta}$. We therefore expect for sodium at much higher Rayleigh numbers than considered here that a profile of $f_{\varepsilon 3\theta}$ may be found which is quite similar to the one found for air: an almost constant value in the centre

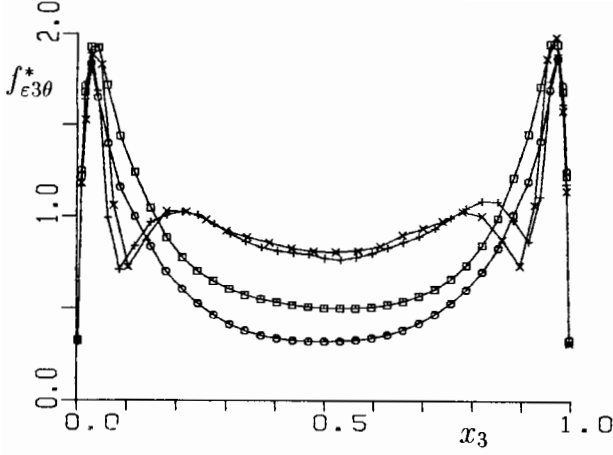


Figure 3: Vertical profile of the value of function $f_{\epsilon 3\theta}^*$ (symbols as in Fig.2.)

of the channel and peaks in the boundary layers. For the parameters considered here, however, the analyzed values of $f_{\epsilon 3\theta}$ do far exceed the expected range $0 \leq f_{\epsilon 3\theta} \leq 1$.

Some turbulence models do not solve a separate transport equation for ϵ_θ . Instead of this, a constant value for the time scale ratio R is prescribed (typically $R \approx 0.85$) and ϵ_θ is calculated directly from (3). However, if we evaluate $f_{\epsilon 3\theta}$ from (2) assuming $R = 0.85 = \text{const.}$, the values and variations of $f_{\epsilon 3\theta}$ become even larger. This result is not surprising since it is well known that R is not a universal constant, but strongly depends on the Prandtl number and the turbulence level, see e.g. Wörner and Grötzbach (1994).

The results achieved up to now suggest that model (2) is not able to describe the molecular destruction of turbulent heat flux in fluids with very different Prandtl numbers in an adequate form. Therefore it seems appropriate to extend model (2) by a term that explicitly accounts for the influence of Pr . Such a model is proposed by Shikazono and Kasagi (1993):

$$\epsilon_{i\theta} = C_\epsilon f_{\epsilon 1} f_{\epsilon 2} \frac{1 + Pr}{2\sqrt{Pr}\sqrt{R}} \frac{\epsilon}{k} \overline{u_i \theta} \quad (4)$$

Here, $f_{\epsilon 1}$ depends on the ratio of energy-dissipating range timescale to energy-containing range timescale, and $f_{\epsilon 2}$ depends on $\sqrt{R/Pr}$. Model (4) was mainly developed for calculation of scalar transport in isotropic and sheared turbulence. Nevertheless, it is worth to investigate its performance for pure natural convection. We do not use the formulations for the functions $f_{\epsilon 1}$ and $f_{\epsilon 2}$ given in Shikazono and Kasagi (1993) but use our direct simulation data to evaluate the product

$$f_{\epsilon 3\theta}^* = C_\epsilon f_{\epsilon 1} f_{\epsilon 2} = \frac{2\sqrt{Pr}\sqrt{R}}{1 + Pr} \frac{k}{\overline{u_3 \theta}} \frac{\epsilon_{3\theta}}{\epsilon} \quad (5)$$

The vertical profiles of $f_{\epsilon 3\theta}^*$ are, for the four cases considered above, given in Fig. 3. Now, as the effect of Prandtl number is included directly in model (4) and is no more hidden in $f_{\epsilon i\theta}$, as it is done in model (2), a clear improvement is achieved: the value of $f_{\epsilon 3\theta}^*$ in the centre of the layer is always

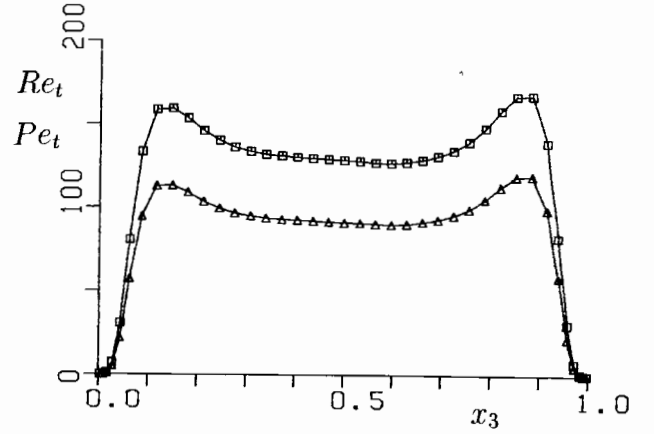


Figure 4: Vertical profile of Re_t (\square) and Pe_t (\triangle) for air ($Ra = 630,000$)

Table 2: Local values of Re_t , Pe_t , and $f_{\epsilon 3\theta}^*$ at $x_3 = 0.5$

Pr	Ra	Re_t	Pe_t	$f_{\epsilon 3\theta}^*$
0.006	3,000	284.4	1.7	0.815
0.006	6,000	595.4	3.6	0.663
0.006	12,000	1,104.1	6.6	0.491
0.006	24,000	1,804.3	10.8	0.321
0.024	3,000	122.2	3.1	0.894
0.024	6,000	432.0	10.8	0.789
0.024	12,000	623.9	15.6	0.643
0.024	25,000	747.3	18.7	0.593
0.024	50,000	974.7	24.4	0.424
0.71	381,000	107.1	76.1	0.809
0.71	630,000	128.3	91.1	0.774

less than unity, regardless of Pr . However, in the boundary layers still sharp peaks are present and $f_{\epsilon 3\theta}^*$ reaches values up to two.

We now investigate the dependence of $f_{\epsilon 3\theta}^*$ on the turbulence Reynolds and Peclet number. As k and ϵ are both functions of the vertical coordinate, Re_t and Pe_t depend on x_3 , too. For the simulation with air and $Ra = 630,000$ the vertical profiles of both quantities show a constant plateau in the centre of the channel and small peaks at the edges of the boundary layers, whereas in the direct vicinity of the walls Re_t and Pe_t approach zero, see Fig.4. For sodium, the profiles of Re_t and Pe_t are qualitatively similar to those found for air, thus they are not shown here. However, because the ratio Pe_t/Re_t equals the Prandtl number, Pe_t and Re_t differ by about two orders of magnitude for liquid metals. Because both, $f_{\epsilon 3\theta}^*$ and Pe_t (or Re_t , respectively) individually depend on x_3 , it is necessary to consider them as local quantities in order to establish a relationship. Here, we select the values of $f_{\epsilon 3\theta}^*$, Pe_t , and Re_t in channel midwidth, i.e. $x_3 = 0.5$, as being representative. The corresponding values are summarized in Table 2.

In Fig. 5, the local values of $f_{\epsilon 3\theta}^*$ are plotted against the local turbulence Peclet number. For each fluid consid-

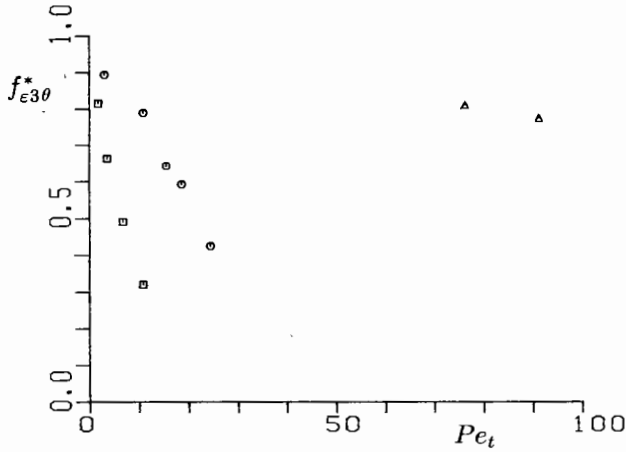


Figure 5: $f_{\epsilon 3\theta}^*$ plotted against Pe_t for sodium (\square), mercury (\circ) and air (\triangle)

ered, $f_{\epsilon 3\theta}^*$ decreases as Pe_t increases. This is reasonable, because with increasing Pe_t (or Re_t , respectively) the molecular terms in the turbulent heat flux equation become less and less important. However, due to the great spreading of the data in Fig. 5 it becomes evident that $f_{\epsilon 3\theta}^*$ does not exclusively depend on Pe_t . If we plot $f_{\epsilon 3\theta}^*$ over Re_t instead of Pe_t , the spreading of the data is clearly reduced. However, the correct scaling for $f_{\epsilon 3\theta}^*$ is the sum of turbulence Reynolds and Peclet number. This is demonstrated in Fig. 6, where all data do almost fall together to one single curve. The result that the sum $Re_t + Pe_t$ is the suitable scaling for $f_{\epsilon 3\theta}^*$ is not very surprising. Note that in the dimensional form of the $u_i\theta$ -equation the factor $(\nu + \kappa)$ enters in $\epsilon_{i\theta}$. Thus both molecular processes, namely friction and conduction, are responsible for generation of $\epsilon_{i\theta}$. To account for both of these molecular effects, Re_t and Pe_t need to be included in a suitable formulation of $f_{\epsilon 3\theta}^*$. This is of special importance if model (4) is intended to be quite general, and thus may be used with fluids which represent a broad range of Pr .

Inspecting Fig. 6, we propose that for natural convection

$$f_{\epsilon 3\theta}^* = \exp(-C_{\epsilon 3\theta} (Re_t + Pe_t)) \quad (6)$$

may be a reasonable approximation for a variety of Rayleigh and Prandtl numbers. Eq. (6) fits best to our direct simulation data if a value $C_{\epsilon 3\theta} \approx 0.0007$ is used, see Fig. 6. In Rayleigh-Bénard convection $\overline{u_1\theta}$ and $\overline{u_2\theta}$ are zero. Therefore we can not evaluate $C_{\epsilon 1\theta}$ and $C_{\epsilon 2\theta}$. Nevertheless, as a first approximation $C_{\epsilon 1\theta} \approx C_{\epsilon 2\theta} \approx C_{\epsilon 3\theta}$ may be used.

Models for the Molecular Diffusion

For flows where Re_t and Pe_t are both high, the molecular diffusion $D_{i\theta,m}$ is of some importance near walls, but outside the boundary layers it is very small as compared to the turbulent part $D_{i\theta,t}$. In turbulence models $D_{i\theta,m}$ is therefore often neglected. If it is modelled at all, usually the following simple approach is adopted (e.g. Shikazono and Kasagi, 1993):

$$D_{i\theta,m} = \frac{\nu + \kappa}{2} \frac{\partial^2 \overline{u_i\theta}}{\partial x_k^2} \quad (7)$$

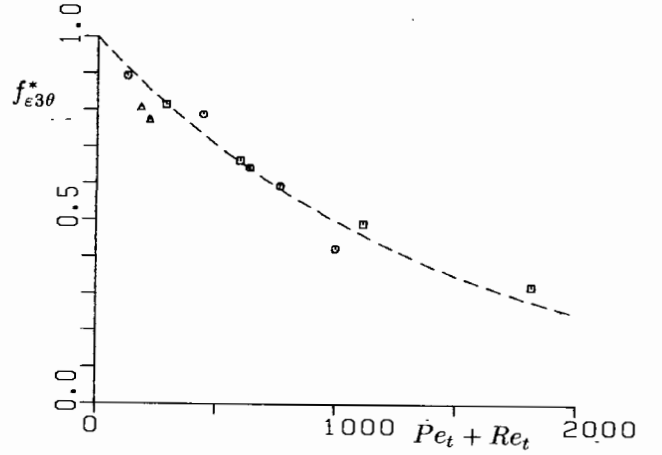


Figure 6: $f_{\epsilon 3\theta}^*$ plotted against $(Pe_t + Re_t)$; symbols as in Fig. 5, dashed line = Eq. (6) with $C_{\epsilon 3\theta} = 0.0007$

Note that in the dimensionless form used in this paper, ν and κ correspond to $1/\sqrt{Gr}$ and $1/(Pr\sqrt{Gr})$, respectively.

Peeters and Henkes (1992) rewrite the molecular diffusion term:

$$D_{i\theta,m} = \frac{\partial}{\partial x_k} \left(\overline{\nu u_i \frac{\partial \theta}{\partial x_k}} + \kappa \theta \frac{\partial u_i}{\partial x_k} \right) = \nu \frac{\partial^2 \overline{u_i\theta}}{\partial x_k^2} + (\kappa - \nu) \overline{u_i \frac{\partial^2 \theta}{\partial x_k^2}} + (\kappa - \nu) \frac{\partial u_i}{\partial x_k} \frac{\partial \theta}{\partial x_k} \quad (8)$$

This derivation is not unique. In a similar way one can obtain a decomposition with κ as a leading term. However, for our purposes where we are mainly interested in low Prandtl number fluids, decomposition (8) is most suitable.

From (8) we see that for a fluid with $Pr = 1$ Eq. (7) is an exact representation of $D_{i\theta,m}$. However, in fluids where the Prandtl number is far from unity, and thus ν and κ differ considerably, a simple averaging of both molecular transport coefficients seems not to be justified, as may be concluded from our results obtained above.

As for such fluids adequate modelling of both, the molecular destruction and molecular diffusion is essential, we propose a different approach for modelling the molecular terms in the turbulent heat flux equation. Instead of approximating both terms by separate models, e.g. (4) and (7), we suggest to take into account both molecular effects by one single model. Using identity (8) we rewrite the sum of molecular destruction and diffusion and get:

$$\epsilon_{i\theta} + D_{i\theta,m} = \underbrace{\frac{1}{\sqrt{Gr}} \frac{\partial^2 \overline{u_i\theta}}{\partial x_k^2}}_{\Sigma_{i,1}} - \underbrace{\frac{2}{\sqrt{Gr}} \frac{\partial u_i}{\partial x_k} \frac{\partial \theta}{\partial x_k}}_{\Sigma_{i,2}} + \underbrace{\frac{1}{\sqrt{Gr}} \left(\frac{1}{Pr} - 1 \right) \overline{u_i \frac{\partial^2 \theta}{\partial x_k^2}}}_{\Sigma_{i,3}} \quad (9)$$

The first term on the right hand side of (9) may be interpreted as the diffusive transport of $\overline{u_i\theta}$ caused by viscous

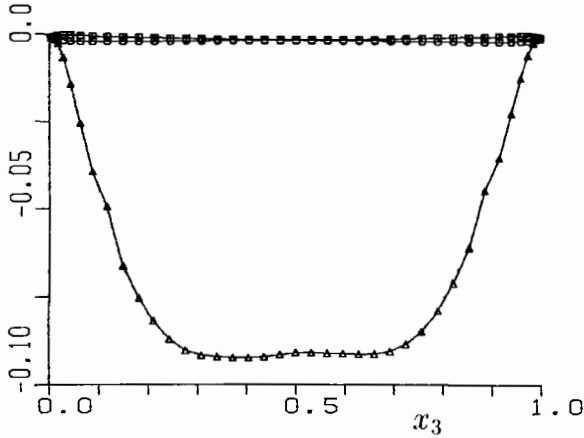


Figure 7: $\Sigma_{3,1}(\square)$, $\Sigma_{3,2}(\circ)$, $\Sigma_{3,3}(\triangle)$ for sodium, $Ra = 24,000$

forces only. It does not require any modelling and can be added to the modelled $\overline{u_i\theta}$ -equation in its original form. The second term on the r.h.s of (9) represents twice the molecular destruction of $\overline{u_i\theta}$ due to viscous forces. It may be modelled by (4) and (6), where for calculation of function $f_{\varepsilon_i\theta}^*$ instead of the sum of turbulence Reynolds and Peclet number $2Re_t$ should be used as argument. The third term on the r.h.s of (9) finally may be interpreted as a representation of the summarized effects in the $\overline{u_i\theta}$ -equation due to thermal conductivity. To authors knowledge, the term $\Sigma_{i,3}$ has not appeared in literature up to now. Thus, its modelling is a task still to be done.

As a first step in this direction, we investigate the magnitude of the three terms on the r.h.s. of (9) and evaluate $\Sigma_{3,1}$, $\Sigma_{3,2}$ and $\Sigma_{3,3}$ from our direct simulation data. In Fig. 7 we give the results for sodium at $Ra = 24,000$. Obviously, $\Sigma_{3,1}$ and $\Sigma_{3,2}$ are almost negligible as compared to $\Sigma_{3,3}$. This just reflects the fact that in liquid metals effects due to thermal conductivity are very important, whereas those due to viscous friction are not really relevant in the $\overline{u_i\theta}$ -equation. The analysis for the simulations with air (not shown here), where $\nu \approx \kappa$, yields the expected result that $\Sigma_{3,1}$, $\Sigma_{3,2}$ and $\Sigma_{3,3}$ are of same magnitude and are all important.

CONCLUSIONS

In this paper we used results of direct numerical simulations of turbulent Rayleigh-Bénard convection in sodium, mercury and air at various Rayleigh numbers and performed a detailed analysis of the molecular terms in the turbulent heat flux equation.

The analyzed budget of $\overline{u_3\theta}$ indicated that due to the anisotropic character of buoyant flows the molecular destruction $\varepsilon_{3\theta}$ is not zero in natural convection, but is an important sink of $\overline{u_3\theta}$, at least for low Reynolds or Peclet number flows. For low Prandtl number fluids redistribution of $\overline{u_3\theta}$ by molecular diffusion $D_{3\theta,m}$ is important, too. Thus, for computation of natural convection adequate modelling of both molecular terms is essential.

From the analysis of conventional models for $\varepsilon_{i\theta}$ two major conclusions can be drawn. First, with respect to the generality of a $\varepsilon_{i\theta}$ -model inclusion of a term is needed which explic-

itly accounts for the influence of Prandtl number. Here, the model proposed by Shikazono and Kasagi (1993) is found to perform quite well. Second, to account for the effect of the turbulence level a model function $f_{\varepsilon_i\theta}^*$ is required. From our results we conclude that this function should be based on the sum of turbulence Reynolds and Peclet numbers. For horizontal fluid layers, an exponential relationship is proposed, see Eq. (6).

For liquid metals we suggested another approach for closure of the molecular destruction and diffusion in the turbulent heat flux equation. It is demonstrated that the effect of both physical processes may be modelled by approximating just one term, namely $\Sigma_{i,3}$ in Eq. (9). However, a model for this term has still to be developed and the feasibility of the present proposal needs to be demonstrated. Finally, we remark that the common modelling of $\varepsilon_{i\theta}$ and $D_{i\theta,m}$ may also be reasonable for high Prandtl number fluids. In this case an expression equivalent to Eq. (9) can be obtained if in rewriting the sum of $\varepsilon_{i\theta}$ and $D_{i\theta,m}$ an identity is used, where κ is the leading term in Eq. (8).

ACKNOWLEDGEMENT

Sincer thanks go to Mr. M. Bunk, who performed the simulations with mercury, and Mr. L. Carteciano for fruitful discussions.

REFERENCES

- Grötzbach, G., 1987, "Direct numerical and large eddy simulation of turbulent channel flows", in: *Encyclopaedia of Fluid Mechanics*, Ed.: N.P. Chermisnoff, Gulf Publ. Houston, Vol.6, pp. 1337-1391.
- Grötzbach, G., 1994, "Direct numerical and large eddy simulation of turbulent heat transfer", *Proceedings, ICHMT Int. Symp. on Turbulence, Heat and Mass Transfer*, Lisbon, Portugal, Vol. 1, pp. I.L.3.1-I.L.3.15.
- Hanjalić, K., 1994, "Achievements and limitations in modelling and computation of buoyant turbulent flow and heat transfer", *Proceedings, 10th Int. Heat Transfer Conference*, Brighton, U.K., Vol. 1, pp. 1-18.
- Peeters, T. W. J., and Henkes, R. A. W. M., 1992, "The Reynolds-stress model of turbulence applied to the natural-convection boundary layer along a heated vertical plate", *Int. J. Heat Mass Transfer*, Vol. 35, pp. 403-420.
- Shikazono N., and Kasagi, N., 1993, "Modeling Prandtl number influence on scalar transport in isotropic and sheared turbulence", *Proceedings, 9th Symp. on Turbulent Shear Flows*, Kyoto, Japan, Vol. 2, pp. 18.3.1 -18.3.6.
- Wörner, M., and Grötzbach, G., 1993a, "Analysis of diffusion of turbulent kinetic energy by direct numerical simulations of natural convection in liquid metals", *Proceedings, NURETH-6*, Grenoble, France, Vol. 1, pp. 186-193.
- Wörner, M., and Grötzbach, G., 1993b, "Turbulent heat flux balance for natural convection in air and sodium analysed by direct numerical simulations", *Proceedings, 5th Int. Symp. on Refined Flow Modelling and Measurements*, Paris, France, pp. 335-342.
- Wörner, M., and Grötzbach, G., 1994, "Analysis of thermal variance equation for natural convection of air and sodium", *Proceedings, ICHMT Int. Symp. on Turbulence, Heat and Mass Transfer*, Lisbon, Portugal, Vol. 1, pp. 9.3.1-9.3.6.